

MVP: MOTION VECTOR PROPAGATION FOR ZERO-SHOT VIDEO OBJECT DETECTION

Binhua Huang[†], Ni Wang[‡], Wendong Yao[†], Soumyabrata Dev[†]

[†]School of Computer Science, University College Dublin

[‡]Amazon Development Center Germany GmbH, Berlin, Germany

ABSTRACT

Running a large open-vocabulary (Open-vocab) detector on every video frame is accurate but expensive. We introduce a training-free pipeline that invokes OWLv2 only on fixed-interval keyframes and propagates detections to intermediate frames using compressed-domain motion vectors (MV). A simple 3×3 grid aggregation of motion vectors provides translation and uniform-scale updates, augmented with an area-growth check and an optional single-class switch. The method requires no labels, no fine-tuning, and uses the same prompt list for all open-vocabulary methods. On ILSVRC2015-VID (validation dataset), our approach (MVP) attains $\text{mAP}@0.5 = 0.609$ and $\text{mAP}@[0.5:0.95] = 0.316$. At loose intersection-over-union (IoU) thresholds it remains close to framewise OWLv2-Large ($0.747/0.721$ at $0.2/0.3$ versus $0.784/0.780$), reflecting that coarse localization is largely preserved. Under the same keyframe schedule, MVP outperforms tracker-based propagation (MOSSE, KCF, CSRT) at $\text{mAP}@0.5$. A supervised reference (YOLOv12x) reaches 0.631 at $\text{mAP}@0.5$ but requires labeled training, whereas our method remains label-free and open-vocabulary. These results indicate that compressed-domain propagation is a practical way to reduce detector invocations while keeping strong zero-shot coverage in videos. Our code and models are available at <https://github.com/microa/MVP>.

Index Terms— Open-vocabulary detection, zero-shot learning, video object detection, compressed-domain inference, motion vectors.

1. INTRODUCTION

Recent reports estimate that modern networks transmit enormous volumes of video every minute, placing heavy demands on automated video analytics [1]. Among many tasks, video object detection is central to content moderation, intelligent traffic monitoring, and high-level scene understanding. However, adapting conventional object detectors that are designed for static images to the dynamics of video can be prohibitively expensive. Classic video pipelines either require retraining on large, domain-specific datasets [2] or depend on temporal modules such as optical flow and sequence-level aggregation [3, 4], which improve robustness but add significant

runtime and often reduce generalization across domains.

In parallel, open-vocabulary detection relaxes the closed-set assumption by transferring semantics from large-scale vision and language pretraining. Representative approaches include CLIP and its detection adaptations such as ViLD, Detic, and RegionCLIP [5–8]. OWLv2 [9] further delivers strong zero-shot detection without task-specific fine-tuning [9]. Despite this progress, running a large open-vocabulary detector on every video frame remains impractical in long videos or on edge devices because the per-frame inference cost is high even without additional training.

A complementary line of research reduces computation by exploiting signals that are already present in compressed video. Modern codecs such as H.264 provide motion vectors and residuals that can be repurposed to propagate features or boxes between sparse keyframes, avoiding explicit optical flow and heavy per-frame inference [10–12]. Many of these methods, however, assume closed vocabularies or require some training on the target dataset. As a result, a simple training-free recipe that unifies open-vocabulary generality with efficient video inference remains underexplored.

This work. We present a training-free and end-to-end pipeline that combines a pretrained open-vocabulary detector (OWLv2) with a lightweight Motion Vector Propagation (MVP) module. The detector is invoked only on fixed-interval keyframes (every K frames). For intermediate frames, MVP reads codec motion vectors to propagate and gently refine bounding boxes [10, 12]. The design needs no additional labels or fine-tuning, cuts the number of expensive detector calls, and preserves strong coarse detection quality across diverse scenes. In experiments, the fixed keyframe schedule recovers much of the framewise baseline at loose IoUs with an expected drop at tight IoUs due to propagation error, and it outperforms classical tracker-based propagation under the same schedule.

Contributions.

- **Training-free and plug-and-play.** A video detection pipeline that requires no additional training or fine-tuning and can be deployed on new datasets without labeled data.
- **Fixed-interval keyframe scheduling with codec-driven propagation.** Per-frame detection is replaced

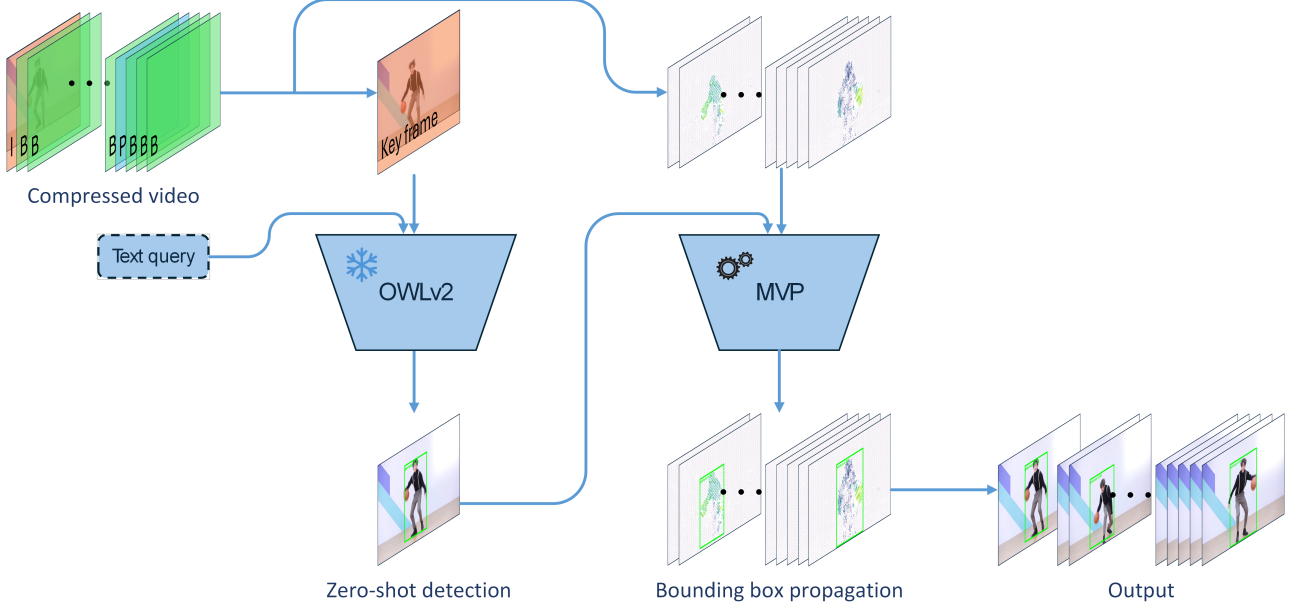


Fig. 1. Overview of the proposed pipeline. Given a compressed video with I-frames and P/B-frames, we select keyframes at a fixed interval (every K frames) and apply OWLv2 [9] with a text prompt to obtain zero-shot detections. For intermediate frames, the MVP module uses codec motion vectors to propagate, adjust, and refine bounding boxes [10, 12]. This schedule reduces expensive detector calls while maintaining competitive detection quality, enabling a training-free and efficient open-vocabulary video detector.

by keyframes every K frames, while compressed-domain motion cues propagate boxes across intermediate frames, reducing computation and retaining competitive accuracy [10–12].

- **Robust propagation techniques.** A practical combination of a 3×3 grid matching strategy, an area-growth check, and a single-class detection mode stabilizes tracks and mitigates drift without supervision.

The proposed approach offers a practical path toward scalable, label-free video understanding by unifying open-vocabulary detection [5–9] with compressed-domain motion [10–12], matching the growth and diversity of real-world video.

2. METHOD

We build a training-free zero-shot video detector by combining a pretrained OWLv2 with a lightweight Motion Vector Propagation (MVP) rule. Keyframes are processed by OWLv2, and intermediate frames update boxes using codec motion vectors. This section specifies the representation, the propagation tests, and the fallback and single-class switches in compact mathematical form. All displays use a unified small size, and only overflow formulas shrink to the column width.

Setup and schedule. Let frames be I_0, \dots, I_{T-1} with image size (W, H) . Let C be the set of text categories. We choose

a fixed keyframe interval K . Denote detections at time t by $D_t = \{(b_n^{(t)}, s_n^{(t)}, c_n^{(t)})\}_n$ where each box $b = (x_c, y_c, w, h)$ follows the YOLO format [13] in $[0, 1]^4$, score $s \in [0, 1]$, and class $c \in C$. Let $S_t \in \{0, 1\}$ denote the single-class switch and q_t the active prompt set:

$$q_t = \begin{cases} \{c^\dagger\} & \text{if } S_t = 1 \text{ with current class } c^\dagger, \\ C & \text{if } S_t = 0. \end{cases}$$

Per-box states. All MVP updates (translation and scale tests, area-growth checks, and fallbacks) are applied independently to each detection n in D_{t-1} , maintaining per-box states (t_n^*, A_n^*) . The detector is invoked according to

$$D_t = \begin{cases} \text{OWLv2}(I_t, q_t) & \text{if } (t \bmod K = 0) \text{ or } \exists n : \text{fallback}_n(t), \\ \mathcal{P}(D_{t-1}, \text{MV}(t)) & \text{otherwise,} \end{cases}$$

where \mathcal{P} is the MVP update using motion vectors at time t .

Pixel-YOLO conversions. For a pixel box $b_{\text{pix}} = (x_{\min}, y_{\min}, x_{\max}, y_{\max})$, define the mapping to YOLO coordinates and its inverse.

$$\Gamma(b_{\text{pix}}; W, H) = \begin{pmatrix} \frac{x_{\min} + x_{\max}}{2W} \\ \frac{y_{\min} + y_{\max}}{2H} \\ \frac{x_{\max} - x_{\min}}{W} \\ \frac{y_{\max} - y_{\min}}{H} \end{pmatrix} = \begin{pmatrix} x_c \\ y_c \\ w \\ h \end{pmatrix}, \quad \Gamma^{-1}\left(\begin{pmatrix} x_c \\ y_c \\ w \\ h \end{pmatrix}\right) : \begin{cases} x_{\min} = W(x_c - \frac{w}{2}), & x_{\max} = W(x_c + \frac{w}{2}), \\ y_{\min} = H(y_c - \frac{h}{2}), & y_{\max} = H(y_c + \frac{h}{2}). \end{cases}$$

3x3 MV Aggregation. Given a previous box $b^{(t-1)}$, let $\Omega(b^{(t-1)})$ be its pixel support and partition it into a 3×3 uniform grid with cell indices $(i, j) \in \{1, 2, 3\}^2$. For each

cell, collect motion vectors whose reference-block centers fall inside, and compute the average:

$$\bar{d}_{ij} = (\bar{u}_{ij}, \bar{v}_{ij}) = \frac{1}{|\mathcal{V}_{ij}|} \sum_{(u,v) \in \mathcal{V}_{ij}} (u, v) \text{ (pixels).}$$

Let $\mathcal{S} = \{(i, j) \mid |\mathcal{V}_{ij}| > 0\}$. We compute the mean translation over non-empty cells

$$\bar{d} = \frac{1}{|\mathcal{S}|} \sum_{(i,j) \in \mathcal{S}} \bar{d}_{ij}, \quad \sigma_{\text{tr}}^2 = \frac{1}{|\mathcal{S}|} \sum_{(i,j) \in \mathcal{S}} \|\bar{d}_{ij} - \bar{d}\|_2^2.$$

Cells with $|\mathcal{V}_{ij}| = 0$ are skipped when computing \bar{d} , σ_{tr} , and statistics of scale ratios (e.g., μ_r , σ_r). We also use a small $\varepsilon > 0$ to avoid division by zero in r_{ij} . If $|\mathcal{S}| = 0$, declare propagation failure.

Translation test. If $\sigma_{\text{tr}} \leq \tau_{\text{tr}}$, apply a pure translation to the box center:

$$\begin{aligned} x_c^{(t)} &= x_c^{(t-1)} + \bar{u}/W, & y_c^{(t)} &= y_c^{(t-1)} + \bar{v}/H, \\ w^{(t)} &= w^{(t-1)}, & h^{(t)} &= h^{(t-1)}. \end{aligned}$$

Uniform-scale test. If the translation test fails, compute cell centers g_{ij} relative to the box center in pixels, and their shifted versions $g'_{ij} = g_{ij} + \bar{d}_{ij}$. With a small $\varepsilon > 0$, define the per-cell *scale ratios* and statistics as:

$$r_{ij} = \frac{\|g'_{ij}\|_2}{\|g_{ij}\|_2 + \varepsilon}, \quad \mu_r = \frac{1}{|\mathcal{S}|} \sum_{(i,j) \in \mathcal{S}} r_{ij}, \quad \sigma_r^2 = \frac{1}{|\mathcal{S}|} \sum_{(i,j) \in \mathcal{S}} (r_{ij} - \mu_r)^2.$$

If $\sigma_r \leq \tau_{\text{sc}}$, update scale and center by the average translation:

$$\begin{aligned} w^{(t)} &= \mu_r w^{(t-1)}, & h^{(t)} &= \mu_r h^{(t-1)}, \\ x_c^{(t)} &= x_c^{(t-1)} + \bar{u}/W, & y_c^{(t)} &= y_c^{(t-1)} + \bar{v}/H. \end{aligned}$$

Propagation failure and fallback. If neither test is accepted, declare propagation failure at time t and call OWLv2. Even if a test passes, apply an area-growth check to prevent explosion. Let

$$A(b) = WH \cdot wh, \quad \text{fallback}_n(t) = [A(b_n^{(t)}) > 2A_n^* \text{ and } (t - t_n^*) \leq 10],$$

$$\text{on fallback (box } n) = (t_n^* \leftarrow t, A_n^* \leftarrow A(b_n^{(t)})).$$

These thresholds were set conservatively based on common motion heuristics to prevent rapid, unrealistic bounding box growth within a short time window, and were not tuned on the target dataset.

Single-class switch. After any OWLv2 call, if and only if there is exactly one detection with score $s \geq \tau_{\text{cls}}$, set $S_t = 1$ and set c^\dagger to that class for subsequent prompts; otherwise set $S_t = 0$. During single-class mode, if OWLv2 fallback occurs and returns empty or scores below τ_{cls} for M consecutive frames, we reset $S_t = 0$.

Clipping and validity. After any update, clip $\Gamma^{-1}(b; W, H)$ to the image bounds, drop boxes with invalid extent or near-zero area, and re-normalize by Γ back to YOLO coordinates.

Components for ablation. We ablate two toggles—(i) *3x3 Grid MV aggregation* and (ii) the *area-growth consistency check*—while keeping the single-class mode *on* unless otherwise noted. Table 4 merges configurations (\checkmark/\times) and results; directory names from our logs are shown for reproducibility.

3. EXPERIMENTS

We evaluate on the ILSVRC2015-VID validation set [14] with its 30 categories. All open-vocabulary methods use the same list of class prompts (OWLv2 [9], YOLO-world [15], and our MVP). Supervised YOLOv12 [16] models use their predefined label sets and do not use text prompts. Our approach is training-free and does not fine-tune on this dataset. We report mAP at four IoU settings: 0.2, 0.3, 0.5, and [0.5:0.95] [17], together with throughput in frames per second (FPS) measured on RTX 3090 when available.

Baselines. Framewise OWLv2 [9] (Large and Base) as open-vocabulary detectors; YOLO-world as a zero-shot detector; the *YOLOv12 family* (s/m/l/x) as supervised references; and classical object trackers (MOSSE, KCF, CSRT) used as propagation modules between sparse keyframes.

Main results. Table 1 compares accuracy, speed, and capability. Framewise OWLv2-Large achieves the strongest accuracy. Our method (MVP) is close at loose IoUs while reducing detector invocations, and reaches 10.3 FPS on RTX 3090. Within the YOLOv12 family, accuracy and speed scale with model size from s to x as expected. OWLv2-Base in this run covers fewer images than other rows and is therefore not strictly comparable; we keep it only as a sanity check.

Fixed keyframe interval. We also evaluate OWLv2-Large under a fixed keyframe interval K (Table 2). At each keyframe we run the detector; on intermediate frames we simply *reuse* the bounding boxes predicted at the most recent keyframe with positions held fixed (“frozen boxes”, no motion compensation). As K grows, this frozen-box baseline trades accuracy—especially at tight IoUs—for higher FPS. By contrast, MVP propagates boxes using motion cues, preserving coarse localization while avoiding the sharp drop.

Propagation module comparison. Under the same keyframe schedule, replacing MVP with classical trackers degrades mAP at all IoUs and lowers throughput.

Ablation. We ablate two toggles—(i) *3x3 Grid MV aggregation* and (ii) the *area-growth check*—while keeping the single-class mode *on* unless otherwise noted. Table 4 merges configurations (\checkmark/\times) and results; directory names from our logs are shown for reproducibility.

Takeaways. (1) Framewise OWLv2-Large is the accuracy upper bound. (2) MVP preserves most coarse detections at 0.2 and 0.3 with an expected drop at tight IoUs. (3) Under the same schedule, MVP is stronger and faster than tracker-based propagation. (4) Fixed-interval sampling shows a clear accuracy versus interval tradeoff; MVP avoids the large loss seen with very sparse detection while keeping double-digit FPS. (5) Within the YOLOv12 family, accuracy and FPS scale with model size; these supervised baselines require labeled training, whereas MVP is training-free and open-vocabulary.

Table 1. Comparison on ILSVRC2015-VID (val). We report four mAPs and FPS (RTX 3090).

Method	mAP@0.2 (↑)	mAP@0.3 (↑)	mAP@0.5 (↑)	mAP@[0.5:0.95] (↑)	FPS (↑)	Category space	Training mode
YOLOv12s [16]	0.556	0.551	0.521	0.379	41	Closed-set	Supervised
YOLOv12m [16]	0.597	0.594	0.569	0.423	39	Closed-set	Supervised
YOLOv12l [16]	0.604	0.599	0.570	0.422	37	Closed-set	Supervised
YOLOv12x [16]	0.651	0.648	0.631	0.485	36	Closed-set	Supervised
YOLO-world [15]	0.323	0.322	0.316	0.247	40	Open-vocab	Zero-shot
OWLv2-Base [9]	0.698	0.694	0.676	0.520	1.5	Open-vocab	Zero-shot
OWLv2-Large [9]	0.784	0.780	0.760	0.552	0.8	Open-vocab	Zero-shot
MVP (ours)	0.747	0.721	0.609	0.316	10.3	Open-vocab	Zero-shot

Notes. (↑) higher is better. FPS values are measured on RTX 3090 under our unified protocol. *Closed-set* refers to conventional detectors trained and evaluated on a fixed set of categories (e.g., the 30 classes of ILSVRC2015-VID). *Supervised* means these models require category-specific annotated training data. In contrast, *Open-vocab* denotes the ability to detect arbitrary categories specified by free-form text prompts, and *Zero-shot* means such generalization is achieved without any task-specific training. Together, open-vocabulary and zero-shot capability represent a fundamental leap beyond closed-set supervised detection, enabling recognition of unseen objects without costly manual annotation.

Table 2. OWLv2-Large at fixed intervals (K) versus our MVP, with FPS on RTX 3090.

Strategy	mAP@0.2	mAP@0.3	mAP@0.5	mAP@[0.5:0.95]	FPS
Every 5 frames	0.604	0.602	0.590	0.428	3.2
Every 10 frames	0.544	0.543	0.531	0.371	5.4
Every 30 frames	0.461	0.458	0.435	0.275	11.1
Every 50 frames	0.416	0.411	0.379	0.226	11.3
MVP (ours)	0.747	0.721	0.609	0.316	10.3

Table 3. Propagation with classical trackers versus MVP, with FPS on RTX 3090.

Method	mAP@0.2	mAP@0.3	mAP@0.5	mAP@[0.5:0.95]	FPS
MOSSE [18]	0.629	0.574	0.426	0.205	4.8
KCF [19]	0.684	0.646	0.513	0.248	4.8
CSRT [20]	0.620	0.558	0.395	0.180	6.6
MVP (ours)	0.747	0.721	0.609	0.316	10.3

4. DISCUSSION AND CONCLUSION

Our results indicate that a training-free, zero-shot video detector is practical when paired with compressed-domain motion. Invoking OWLv2 [9] at fixed keyframe intervals and propagating boxes with codec motion vectors retains much of the framewise detector coarse localization while reducing redundant inference.

Discussion. Prompted OWLv2 provides broad category coverage without dataset-specific training, detecting classes absent from conventional supervised label spaces. Under matched keyframe intervals, MVP remains close to framewise OWLv2-Large at loose IoUs (0.2/0.3) but, as expected for propagation, degrades at tight IoUs; thus it is suitable when coarse localization suffices or compute is constrained. Under the same schedule, MVP outperforms classical tracker propagation (MOSSE, KCF, CSRT) in mAP across IoUs; tracker rows serve as sanity checks, not primary baselines. Supervised baselines (YOLOv12s/m1 on ImageNet-VID) may surpass MVP at IoU 0.5, but require labels and lack open-vocabulary capability.

Table 4. Ablation of MVP components on ILSVRC2015-VID (val). A ✓ means the component is enabled. FPS is wall-clock on RTX 3090 including decoding, MV access, preprocessing, and non-maximum suppression (NMS).

Setting	3x3 Grid MV	Area-growth	Single-class	mAP@0.2	mAP@0.3	mAP@0.5	mAP@[0.5:0.95]	FPS
w/o Single-class check	✓		✗	0.747	0.721	0.609	0.316	10.1
w/o Area-growth check	✓	✗	✓	0.736	0.710	0.601	0.315	10.3
w/o 3x3 Grid MV	✗	✓	✓	0.524	0.460	0.309	0.136	25.0
MVP (full)	✓	✓	✓	0.747	0.721	0.609	0.316	10.3

Notes. Disabling the single-class switch changed FPS by < 2% and left mAP unchanged in our setup (30-class prompts with text-embedding caching); we include the row here for completeness.

Limitations. The approach depends on the quality of codec motion vectors: heavy compression, very low resolution, strong camera motion, or complex deformation can introduce noise and trigger more frequent re-detections. High-precision localization of small or fast-deforming objects, and scenes with large parallax, remains challenging when relying only on translation and uniform scaling. Prompt design is also important, since overly broad or poorly calibrated prompts may increase false positives or cause unnecessary fallbacks.

Future work. We plan to explore content-aware keyframe scheduling with lightweight compressed-domain signals; stronger propagation via multi-grid models, residual cues, or confidence-aware fusion to improve tight-IoU accuracy while remaining training-free; simple re-identification to maintain long-range consistency after occlusion; and prompt calibration or automatic prompt expansion to stabilize open-vocabulary coverage over long clips.

Conclusion. We presented a training-free, open-vocabulary video detector that couples OWLv2 with motion-aware propagation at fixed keyframe intervals. On ILSVRC2015-VID, the method preserves much of the framewise accuracy at loose IoUs, consistently surpasses tracker-based propagation under the same schedule, and requires no additional labels or fine-tuning—making it a practical building block for scalable video understanding when both flexibility and efficiency matter.

5. REFERENCES

[1] Cisco, “Cisco visual networking index: Forecast and trends, 2018–2023,” White paper, Cisco Systems, Inc., June 2020.

[2] Kai Kang, Wanli Ouyang, Hongsheng Li, and Xiaogang Wang, “Object detection from video tubelets with convolutional neural networks,” in *Proceedings of the IEEE conference on computer vision and pattern recognition*, 2016, pp. 817–825.

[3] Xizhou Zhu, Yujie Wang, Jifeng Dai, Lu Yuan, and Yichen Wei, “Flow-guided feature aggregation for video object detection,” in *Proceedings of the IEEE international conference on computer vision*, 2017, pp. 408–417.

[4] Haiping Wu, Yuntao Chen, Naiyan Wang, and Zhaoxiang Zhang, “Sequence level semantics aggregation for video object detection,” in *Proceedings of the IEEE/CVF international conference on computer vision*, 2019, pp. 9217–9225.

[5] Alec Radford, Jong Wook Kim, Chris Hallacy, Aditya Ramesh, Gabriel Goh, Sandhini Agarwal, Girish Sastry, Amanda Askell, Pamela Mishkin, Jack Clark, et al., “Learning transferable visual models from natural language supervision,” in *International conference on machine learning*. PMLR, 2021, pp. 8748–8763.

[6] Xiuye Gu, Tsung-Yi Lin, Weicheng Kuo, and Yin Cui, “Open-vocabulary object detection via vision and language knowledge distillation,” *arXiv preprint arXiv:2104.13921*, 2021.

[7] Xingyi Zhou, Rohit Girdhar, Armand Joulin, Philipp Krähenbühl, and Ishan Misra, “Detecting twenty-thousand classes using image-level supervision,” in *European conference on computer vision*. Springer, 2022, pp. 350–368.

[8] Yiwu Zhong, Jianwei Yang, Pengchuan Zhang, Chunyuan Li, Noel Codella, Liunian Harold Li, Luowei Zhou, Xiyang Dai, Lu Yuan, Yin Li, et al., “Regionclip: Region-based language-image pretraining,” in *Proceedings of the IEEE/CVF conference on computer vision and pattern recognition*, 2022, pp. 16793–16803.

[9] Matthias Minderer, Alexey Gritsenko, and Neil Houlsby, “Scaling open-vocabulary object detection,” *Advances in Neural Information Processing Systems*, vol. 36, pp. 72983–73007, 2023.

[10] Chao-Yuan Wu, Manzil Zaheer, Hexiang Hu, R Manmatha, Alexander J Smola, and Philipp Krähenbühl, “Compressed video action recognition,” in *Proceedings of the IEEE conference on computer vision and pattern recognition*, 2018, pp. 6026–6035.

[11] Mason Liu and Menglong Zhu, “Mobile video object detection with temporally-aware feature maps,” in *Proceedings of the IEEE conference on computer vision and pattern recognition*, 2018, pp. 5686–5695.

[12] Shiyao Wang, Hongchao Lu, and Zhidong Deng, “Fast object detection in compressed video,” in *Proceedings of the IEEE/CVF international conference on computer vision*, 2019, pp. 7104–7113.

[13] Joseph Redmon, Santosh Divvala, Ross Girshick, and Ali Farhadi, “You only look once: Unified, real-time object detection,” in *Proceedings of the IEEE conference on computer vision and pattern recognition*, 2016, pp. 779–788.

[14] Olga Russakovsky, Jia Deng, Hao Su, Jonathan Krause, Sanjeev Satheesh, Sean Ma, Zhiheng Huang, Andrej Karpathy, Aditya Khosla, Michael Bernstein, et al., “Imagenet large scale visual recognition challenge,” *International journal of computer vision*, vol. 115, pp. 211–252, 2015.

[15] Tianheng Cheng, Lin Song, Yixiao Ge, Wenyu Liu, Xinggang Wang, and Ying Shan, “Yolo-world: Real-time open-vocabulary object detection,” in *Proceedings of the IEEE/CVF Conference on Computer Vision and Pattern Recognition*, 2024, pp. 16901–16911.

[16] Yunjie Tian, Qixiang Ye, and David Doermann, “Yolov12: Attention-centric real-time object detectors,” *arXiv preprint arXiv:2502.12524*, 2025.

[17] Tsung-Yi Lin, Michael Maire, Serge Belongie, James Hays, Pietro Perona, Deva Ramanan, Piotr Dollár, and C Lawrence Zitnick, “Microsoft coco: Common objects in context,” in *European conference on computer vision*. Springer, 2014, pp. 740–755.

[18] David S Bolme, J Ross Beveridge, Bruce A Draper, and Yui Man Lui, “Visual object tracking using adaptive correlation filters,” in *2010 IEEE computer society conference on computer vision and pattern recognition*. IEEE, 2010, pp. 2544–2550.

[19] João F Henriques, Rui Caseiro, Pedro Martins, and Jorge Batista, “High-speed tracking with kernelized correlation filters,” *IEEE transactions on pattern analysis and machine intelligence*, vol. 37, no. 3, pp. 583–596, 2014.

[20] Alan Lukezic, Tomas Vojir, Luka Čehovin Zajc, Jiri Matas, and Matej Kristan, “Discriminative correlation filter with channel and spatial reliability,” in *Proceedings of the IEEE conference on computer vision and pattern recognition*, 2017, pp. 6309–6318.